Late-spring frost risk between 1959 and 2017 decreased in North America but increased in Europe and Asia

Constantin M. Zohner[a,1,2], Lidong Mo[a,1], Susanne S. Renner[b], Jens-Christian Svenning[c,d], Yann Vitasse[e], Blas M. Benito[f], Alejandro Ordonez[c,d,g], Frederik Baumgarten[e], Jean-François Bastin[a,h], Veronica Sebald[b], Peter B. Reich[i,j], Jingjing Liang[k], Gert-Jan Nabuurs[l,m], Sergio de-Miguel[n,o], Giorgio Alberti[p,q], Clara Antón-Fernández[r], Radomir Balazy[s], Urs-Beat Brändli[t], Han Y. H. Chen[u,v], Chelsea Chisholm[a], Emil Cienciala[w,x], Selvadurai Dayanandan[y,z], Tom M. Fayle[aa,bb], Lorenzo Frizzera[cc], Damiano Gianelle[cc], Andrzej M. Jagodzinski[dd,ee], Bogdan Jaroszewicz[ff], Tommaso Jucker[gg], Sebastian Kepfer-Rojas[hh], Mohammed Latif Khan[ii], Hyun Seok Kim[jj,kk,ll,mm], Henn Korjus[nn], Vivian Kvist Johannsen[hh], Diana Laarmann[nn], Mait Lang[nn,oo], Tomasz Zawila-Niedzwiecki[pp], Pascal A. Niklaus[qq], Alain Paquette[rr], Hans Pretzsch[ss], Purabi Saikia[tt], Peter Schall[uu], Vladimír Šebeň[vv], Miroslav Svoboda[ww], Elena Tikhonova[xx], Helder Viana[yy,zz], Chunyu Zhang[aaa], Xiuhai Zhao[aaa], and Thomas W. Crowther[a]

Edited by Thomas J. Givnish, University of Wisconsin–Madison, Madison, WI, and accepted by Editorial Board Member Robert E. Dickinson March 30, 2020 (received for review November 29, 2019)

Late-spring frosts (LSFs) affect the performance of plants and animals across the world's temperate and boreal zones, but despite their ecological and economic impact on agriculture and forestry, the geographic distribution and evolutionary impact of these frost events are poorly understood. Here, we analyze LSFs between 1959 and 2017 and the resistance strategies of Northern Hemisphere woody species to infer trees' adaptations for minimizing frost damage to their leaves and to forecast forest vulnerability under the ongoing changes in frost frequencies. Trait values on leaf-out and leaf-freezing resistance come from up to 1,500 temperate and boreal woody species cultivated in common gardens. We find that areas in which LSFs are common, such as eastern North America, harbor tree species with cautious (late-leafing) leaf-out strategies. Areas in which LSFs used to be unlikely, such as broad-leaved forests and shrublands in Europe and Asia, instead harbor opportunistic tree species (quickly reacting to warming air temperatures). LSFs in the latter regions are currently increasing, and given species' innate resistance strategies, we estimate that ∼35% of the European and ∼26% of the Asian temperate forest area, but only ∼10% of the North American, will experience increasing late-frost damage in the future. Our findings reveal region-specific changes in the spring-frost risk that can inform decision-making in land management, forestry, agriculture, and insurance policy.

climate change | phenology | spring leaf-out | late frost | freezing damage

Extreme climate events, such as heat or cold waves, cause large damage to ecosystems (1–3), threatening food security (4–6) and the global economy (7, 8). As the climate warms, extreme events might become more frequent, amplifying the consequences of climate change (9). Late-spring frosts (LSFs), i.e., below-freezing temperatures in late spring, are among the most critical extreme events in temperate and boreal regions (10–12). Tissue damage induced by LSFs greatly affects growth, competitive ability, and distribution limits of plants (1, 10, 11, 13–18). This is because plants are most vulnerable to frosts while their leaves are young (19, 20). In North America and Europe, late-frost damage to crops and trees causes more economic losses to agriculture than any other climate-related hazards (21, 22). A single LSF across Europe in spring 2017 resulted in economic losses of 3.3 billion euros, of which only 18% were insured (23). Besides negative consequences for agriculture and forestry, extensive plant frost damage contributes to the increase in atmospheric CO_2 levels as a result of decreased photosynthesis (24, 25). Quantitative and spatially explicit information about the extent and severity of LSFs is thus essential to guide climate modeling (24, 26, 27), agriculture, forestry, and environmental decision-making (21). Yet, we still lack even a basic understanding of broad-scale biogeographic and temporal patterns in LSFs.

To assess the vulnerability of forests to frost events under climate change, we need to analyze not only the distribution of LSFs in space and time but also the resistance of trees to frost

Significance

Frost in late spring causes severe ecosystem damage in temperate and boreal regions. We here analyze late-spring frost occurrences between 1959 and 2017 and woody species' resistance strategies to forecast forest vulnerability under climate change. Leaf-out phenology and leaf-freezing resistance data come from up to 1,500 species cultivated in common gardens. The greatest increase in leaf-damaging spring frost has occurred in Europe and East Asia, where species are more vulnerable to spring frost than in North America. The data imply that 35 and 26% of Europe's and Asia's forests are increasingly threatened by frost damage, while this is only true for 10% of North America. Phenological strategies that helped trees tolerate past frost frequencies will thus be increasingly mismatched to future conditions

Author contributions: C.M.Z. conceived and developed the study with input from S.S.R. and J.-C.S.; C.M.Z. and L.M. performed research; L.M., B.M.B., and A.O. computed the frost risk maps; C.M.Z. and V.S. collected the phenology and leaf freezing resistance data; C.M.Z. wrote the manuscript with assistance from S.S.R. and T.W.C.; Y.V., B.M.B., A.O., F.B., J.-F.B., V.S., P.B.R., and J.L. provided input on the manuscript text; P.B.R., G.-J.N., S.d.-M., G.A., C.A.-F., R.B., U.-B.B., H.Y.H.C., C.C., E.C., S.D., T.M.F., L.F., D.G., A.M.J., B.J., T.J., S.K.-R., M.L.K., H.S.K., H.K., V.K.J., D.L., M.L., T.Z.-N., P.A.N., A.P., H.P., P. Saikia, P. Schall, V.Š., M.S., E.T., H.V., C.Z., and X.Z. contributed forest inventory data; and all authors reviewed the manuscript.

The authors declare no competing interest.

This article is a PNAS Direct Submission. T.J.G. is a guest editor invited by the Editorial Board.

Data deposition: All source code, models, and raw data have been deposited in GitHub (https://github.com/LidongMo/FrostRiskProject) and Datasets S1–S3.

[1]C.M.Z. and L.M. contributed equally to this work.

[2]To whom correspondence may be addressed. Email: constantin.zohner@t-online.de.

This article contains supporting information online at https://www.pnas.org/lookup/suppl/doi:10.1073/pnas.1920816117/-/DCSupplemental.

First published May 11, 2020.

damage to their young leaves. That is, in addition to identifying the regions that are most likely to experience LSFs, understanding tree vulnerability also requires that we document the biogeographic distribution of traits that govern the susceptibility to late frosts (28). Pairing annual frost occurrence and plant trait information will allow identifying the areas where trees are most vulnerable and to forecast the impact of LSFs on plant performance.

The sensitivity of trees and shrubs to LSFs is determined by the freezing resistance of their young leaves and their phenological strategy, that is, how soon after the first spring warming they leaf-out. Species with "cautious" phenological strategies that do not leaf-out unless they have experienced sufficient winter chilling and/or day lengths, regardless of short warm spells in spring, should be favored in areas with frequent severe LSFs (29, 30). By contrast, "opportunistic" species that leaf-out early, even after short periods of warming, should be common in areas where phenological tracking of spring temperature carries no risk because LSFs are unlikely (31). Those forests and shrublands harboring the highest proportions of phenologically opportunistic species with low leaf-freezing resistance should be the most vulnerable to late-frost damage if the severity of LSFs is increasing with climate change.

Here, we test if a high likelihood of LSFs has led to cautious phenological characteristics and whether there are therefore differences among regional forests and shrublands in their vulnerability to late-frost damage. To do this, we created spatially explicit maps of the leaf-out strategies and leaf-freezing resistance of numerous woody species and related them to the spring climate between 1959 and 2017. Our exploration of the geographic distribution of these plant traits is based on a forest-biodiversity dataset combined with common-garden data for up to 1,500 species.

To map LSFs between 1959 and 2017 across the world's temperate and boreal regions, we calculated the amount of warming (growing-degree days >0 °C) accumulated before the last spring freezing event (<0 °C) for each year, using gridded data on daily minimum and mean temperatures (Fig. 1). This measure of spring-frost lateness is necessary because time of year per se is not a useful indicator of LSFs. The more warming a plant receives before the last spring frost, the more time it has to unfold frost-susceptible organs such as leaves and flowers (in whose cells water may freeze), and thus the higher its frost vulnerability. To characterize the global distribution of LSFs, we then calculated the 95% quantiles of the accumulated warming before the last freezing of all years for each pixel (Fig. 1*A*). The 95% quantiles of accumulated warming were chosen to reflect regional LSF because it is the extreme years that determine the likelihood of late-frost events in that region.

Geographic Variation in Late-Spring Frosts

Among our most striking results is that LSFs are generally more severe in North America than in Eurasia (Figs. 1 *A* and *C* and 2). For example, on average, temperate forests in North America experience LSFs after ∼50% more spring warming has occurred than in Europe and East Asia. When using a freezing threshold of −4 °C instead of 0 °C, this difference was even more pronounced (*SI Appendix*, Fig. S1 *A* and *C*); extreme frosts occur in North American temperate forests after twice the spring warmth than in Europe and East Asia. The strong continental-scale differences in LSF match the absence of horizontal mountain ranges in North America, allowing both warm spells from the Gulf of Mexico and cold spells from Arctic regions to move through the continent unimpeded. This results in high short-term temperature variability, with warm periods frequently alternating with freezing temperatures, increasing the likelihood of LSFs across the continent.

The continental-scale differences in LSF (Fig. 1*A*) are best explained by geographic differences in intramonthly temperature variation, seasonal temperature variation, distance from the sea, and elevation (overall R^2 of multivariate linear model including all variables = 0.64; see Fig. 2 for univariate variable effects). LSF declines with increasing latitude. This is because, in cold high-latitude regions, 1) short-term (intradaily to intramonthly) temperature variation is low, leading to a low probability of night frosts when days are warm; and 2) temperature seasonality is high, leading to a faster transition from winter to summer and thus a lower probability of accumulating substantial warming when frost occurrence is still possible. Our results also show that, in contrast to previous suggestions (31), coastal regions do not exhibit more severe LSFs. In fact, for boreal and temperate broadleaf forests, the likelihood of LSFs increases with distance to the sea (Fig. 2), probably because warm ocean currents lower the probability of late frosts in coastal regions. Finally, the likelihood of LSF increases with elevation (Fig. 2), most likely due to higher intradaily temperature variation.

Biogeographic Variation in Plant Traits That Govern Frost Susceptibility

To maximize growing-season length and minimize late-frost damage, plants exhibit locally adapted leaf-out strategies that may also reflect the geographic variation in LSFs. Flora-wide differences in leaf-out strategies were first found in common garden experiments that included up to 1,585 species of temperate and boreal trees, shrubs, and climbers from Asia, Europe, and North America (29, 30). That experimental work, however, did not focus on late-frost damage and resistance strategies to late frost.

To test for correlations between LSF and plant-functional traits and to estimate regional (flora-wide) plant performance, we compiled trait values on leaf-out and leaf-freezing resistance in 1,568 and 354 species, respectively, of temperate and boreal woody taxa cultivated in common gardens and data on their natural occurrences from 534,262 forest and shrubland inventory plots from both the Northern and Southern Hemisphere (*SI Appendix*, Fig. S4). To obtain species-specific leaf-out dates, we averaged leaf-out observations from eight common gardens, located in Eastern North America, Europe, and East Asia, using site-adjustment factors to account for climate differences among sites. As such, the average and interannual variation in leaf-out dates we report here reflect the genotypic, interspecific variation in leaf-out dates when all species are kept under the same conditions and do not show phenotypic differences expressed as a result of environmental forcing in their native habitats. Data on species' leaf-freezing resistance shortly after leaf-out in spring came from observations in two common gardens in Germany (see *Methods* for details).

Using 10 global layers of climate and topography, we extrapolated the relationships between plant traits and environmental variables using random forest models (32) to generate spatially explicit maps of species' leaf-freezing resistance (Fig. 3) and leaf-out strategies (average and interannual variation in leaf-out dates; Fig. 4). Model strength was evaluated individually for four biomes—temperate shrubland, temperate broadleaf/mixed forest, temperate conifer forest, and boreal forests—using R^2 values of observed versus predicted values, including either all measurements or subsets of the data (10-fold cross validation; *SI Appendix*, Fig. S5).

Overall, our models performed well in predicting global trait variation (overall R^2 = 0.94 to 0.97; cross-validation R^2 = 0.17 to 0.76; *SI Appendix*, Fig. S5), although model fit was low when predicting freezing resistance of leaves in boreal regions (cross-validation R^2 = 0.17) probably because of low trait variation among sites in that biome (*SI Appendix*, Fig. S5). Temperature plays a prominent role in shaping the biogeographic

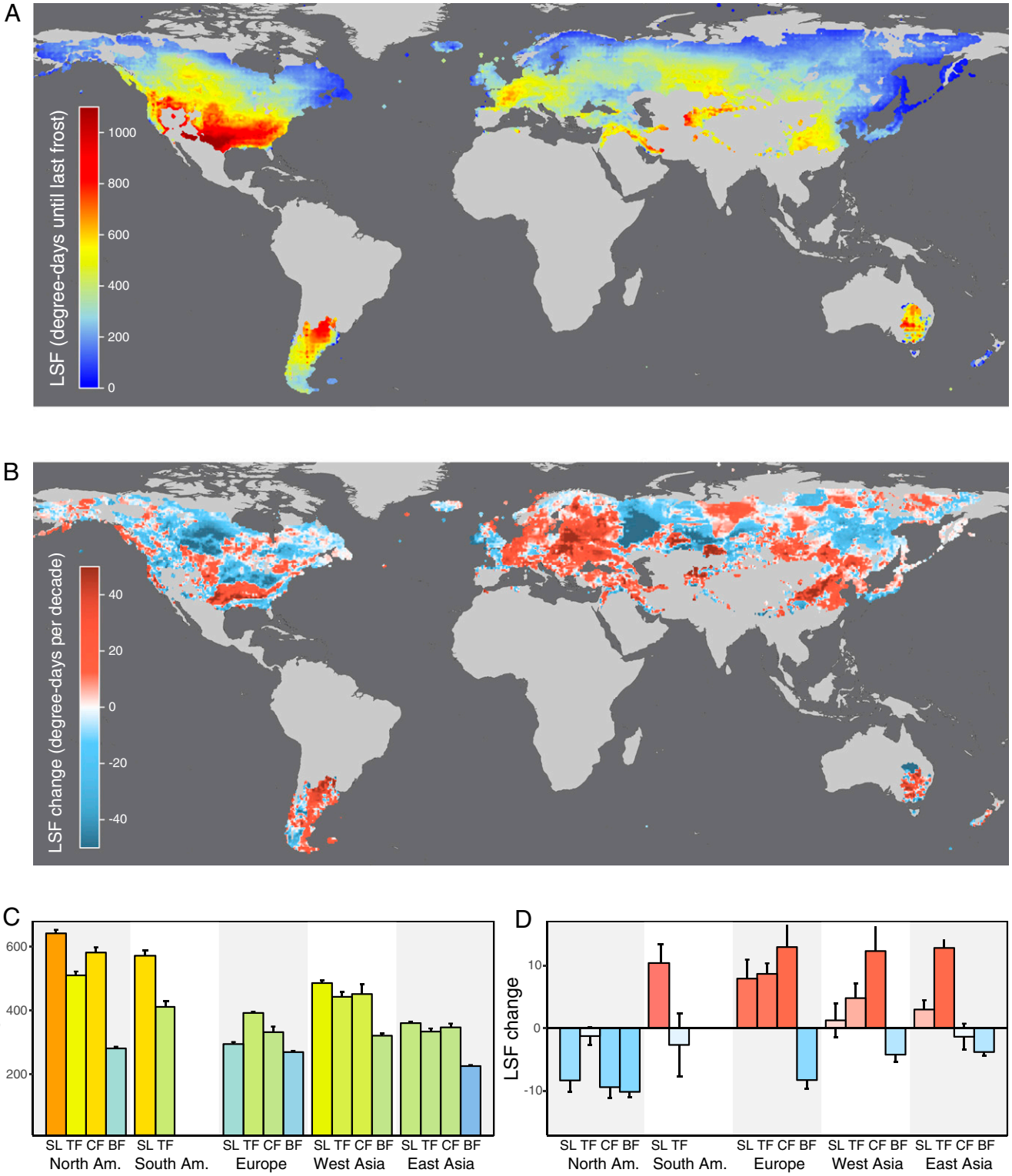

Fig. 1. Global variation in LSF (*A*) and temporal changes in LSF (LSF change) (*B*) between 1959 and 2017 in the world's temperate and boreal regions. (*A*) Map of the 95% quantiles of accumulated growing-degree days (>0 °C) from January 1 (Northern Hemisphere) or July 1 (Southern Hemisphere) until the last frost day (<0 °C) in spring from 1959 to 2017 (LSF) at the 50 × 50 km (30 arc-minutes) pixel scale. (*B*) Map of temporal changes in the maximum number of accumulated growing-degree days until the last frost day in spring from 1959 to 2017 using 10-y moving averages (LSF change). In red and blue areas, the amount of warming until the last frost is increasing and decreasing, respectively. Values reflect the average increase in maximum growing-degree day accumulation until the last frost day per decade. (*C* and *D*) The means ± 95% confidence intervals of LSF (*C*) and LSF change (*D*) per continent and biome type. Color schemes follow *A* and *B*. BF, boreal forest; CF, temperate conifer forest; SL, shrubland; TF, temperate forest (broadleaf/mixed).

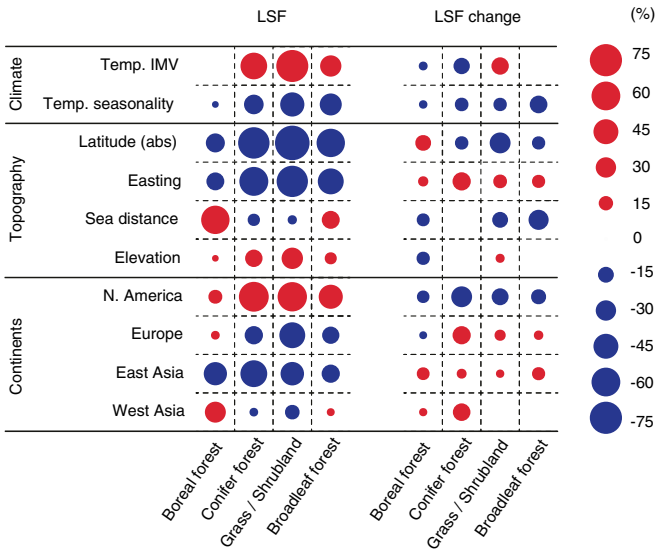

Fig. 2. Standardized coefficients for the effects of climate, topography, and biogeography (continents) on biogeographic variations in LSF and LSF changes over time (LSF change). Coefficients represent relative percentage change in LSF and LSF change for 1 SD increase in the variable (only significant [$P < 0.05$] coefficients are shown). Red and blue circles indicate positive and negative effects, respectively. Circle size indicates the magnitude of effects. All layers are available at the global scale. Elevation and sea distance were square root-transformed for analysis. "Latitude (abs)": absolute latitude (distance from the equator); "Temp. seasonality": temperature annual range (Bioclim7).

patterns in leaf-out strategy and leaf-freezing resistance, which is supported by linear models (*SI Appendix*, Fig. S6). Leaf-freezing resistance predictably declines at lower latitudes (Fig. 3), implying that the costs of freezing resistance outweigh the benefits in warmer regions with longer growing seasons. Importantly, the results show that areas with very late spring frosts harbor species with late leaf-out and low interannual leaf-out variation (Fig. 4 *C* and *D* and *SI Appendix*, Fig. S6), supporting our hypothesis that frequent LSFs favor cautious phenological strategies (i.e., reliance on winter chilling and day length increase, not only warm spring temperatures). The strong imprint of LSF on leaf-out strategy is pinpointed by the differences between North America, Europe, and Asia (Fig. 4 *A* and *B*).

Spatiotemporal Projections of Late-Spring Frost

The impact of future LSFs on plants can be extrapolated from past LSF trajectories and plant traits in the relevant floristic regions and biomes. To do this, we carried out time-series analyses of LSF over the period of 1959 to 2017. Temporal changes were analyzed by moving-window analysis, first calculating the maximum-degree days before the last frost for each 10-y interval (resulting in 50 values per pixel) and then regressing the obtained values against year, using linear regression and Mann-Kendall trend analysis (Fig. 1*B* and *SI Appendix*, Fig. S3). Maximum-degree day values within each 10-y interval were chosen because it is the extreme years that determine regional LSF. We observed similar results when using mean instead of maximum LSF values within each 10-y moving window (Pearson's $r = 0.65$). We also evaluated temporal LSF trajectories using a freezing threshold of −4 °C, which yielded unchanged results for Eurasia but was incongruent with the 0 °C threshold calculation in North America (*SI Appendix*, Figs. S1*F* and S3), underscoring the unpredictability of short-term temperature trends there.

Our results reveal pronounced geographic differences in the temporal trajectories of LSFs (Fig. 1*B*). Across all biomes, LSF has decreased in North America over recent decades, whereas it has increased across most biomes in Europe and Asia, except in boreal forests (Fig. 1 *B* and *D*). Temperate broadleaf forests showed the most pronounced increase in LSF over time, with 65% of the total area covered by this biome experiencing increasing LSF (significant increase in 40% of the total area). In European and East Asian broadleaf forests, increased LSF was found for 70 and 72% of the biome area, respectively (46 and 47% significant). By contrast, in North American broadleaf forests, increased LSF was found for only 50% of the biome area (28% significant).

The most dramatic increase in LSF is occurring in regions where this risk used to be low, such as the coastal and eastern parts of Europe and East Asia (Figs. 1*B* and 2). For a future risk index, we scored areas with a significant increase in LSF (Fig. 1*B*) and that harbor a high proportion of species with

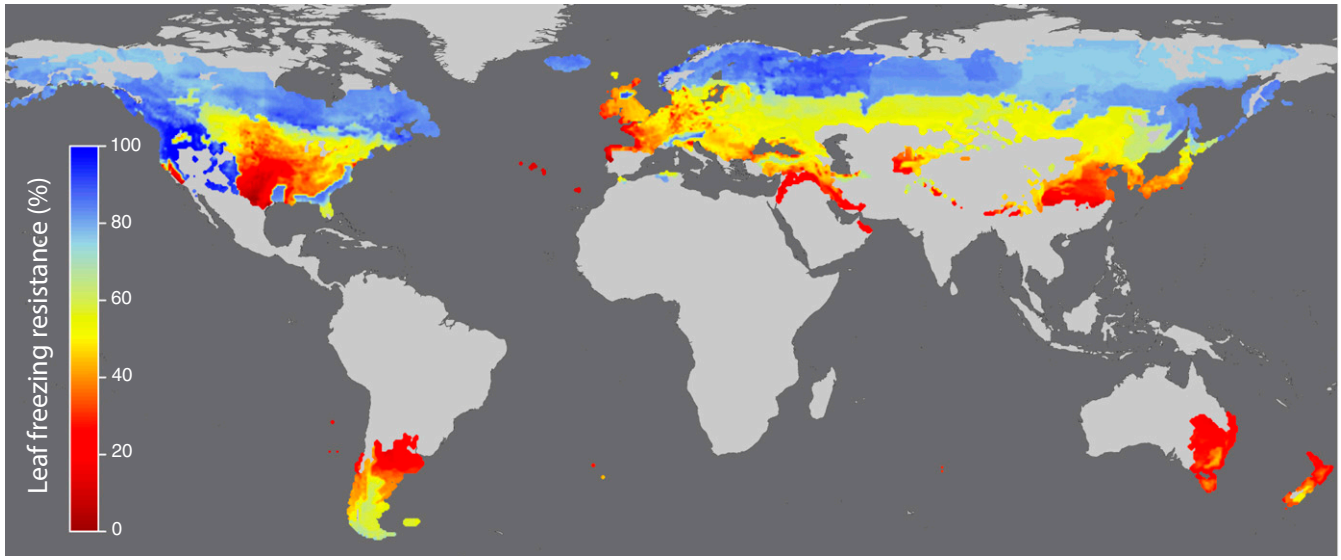

Fig. 3. Global map of tree leaf-freezing resistance in spring. The map shows the percentage of species in a given region with leaves resistant to −4.3 °C frosts shortly after leaf-out for the world's temperate and boreal regions at the 50 × 50 km (30 arc-minutes) pixel scale. See *SI Appendix*, Fig. S5 for model validation.

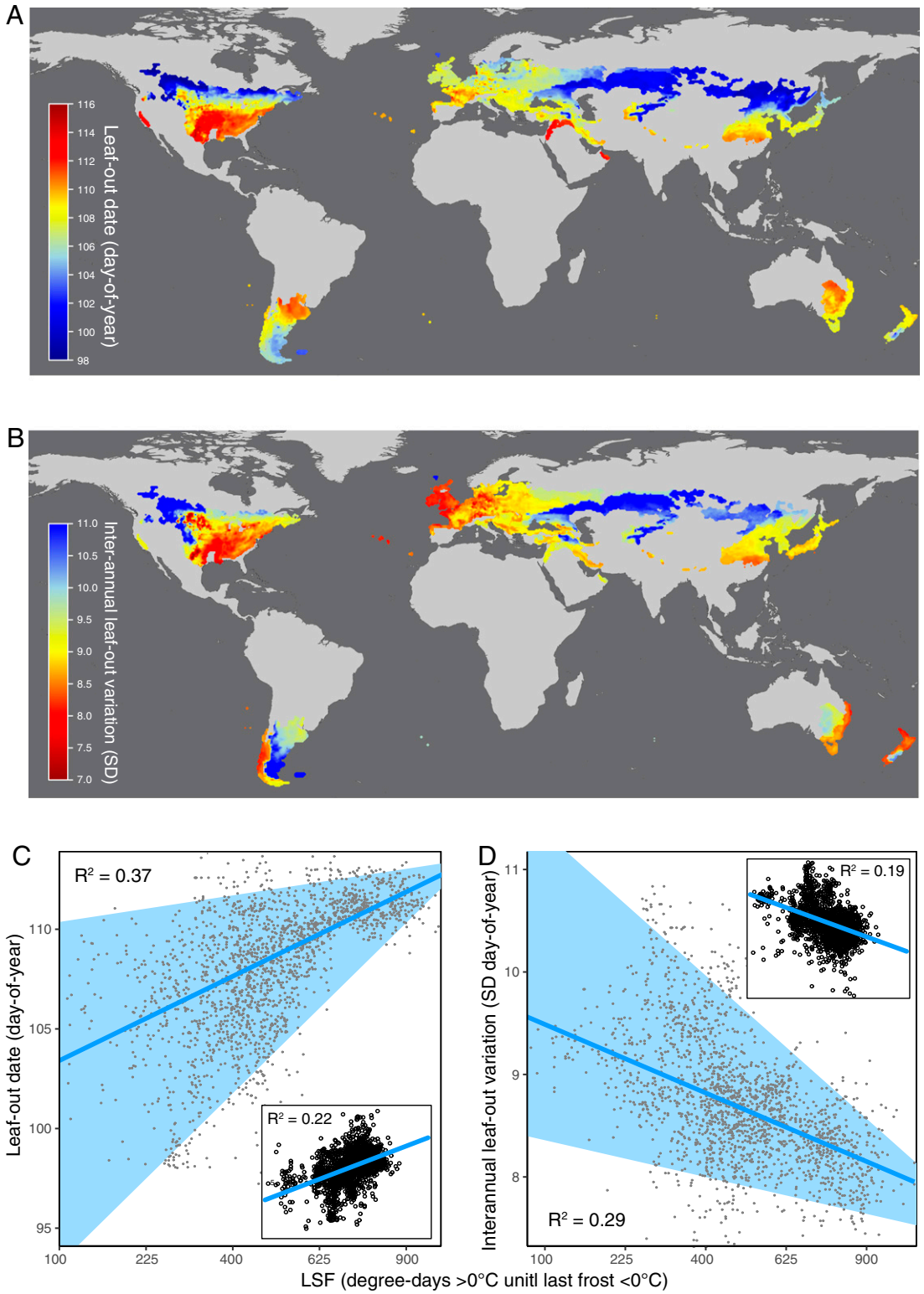

Fig. 4. The effect of LSF on global variation in leaf-out strategies. (*A* and *B*) Global maps of intrinsic differences in leaf-out timing (*A*) and interannual leaf-out variation (*B*) at the 50 × 50 km (30 arc-minutes) pixel scale for temperate forest and shrubland biomes. Leaf-out dates and interannual variation in leaf-out dates were observed under common garden conditions (*Methods*). These maps therefore do not show phenotypic differences expressed as a result of environmental forcing in their native habitats but, rather, show the genotypic (intrinsic) variation in leaf-out strategy. (*C* and *D*) The effect of regional LSF (Fig. 1*A*) on plot-level variation in mean leaf-out date (*C*) and interannual leaf-out variation (*D*) for 1,868 broadleaf forest plots. To analyze how LSF has shaped the phenological strategies of forest communities, we applied quantile regression, showing the 95th quantile (upper limits), the fifth quantile (lower limits), and the 50th quantile (median). The light blue area between the outermost quantiles represents the range of phenological strategies that can be found across the global late-frost risk gradient. Toward regions with pronounced LSFs, the phenological strategies of forests are increasingly restricted to late leaf-out (*C*) and low interannual leaf-out variation (*D*). *Insets* in *C* and *D* show the partial regression between mean leaf-out date and maximum frost risk, controlling for latitude.

opportunistic phenologies (Fig. 4) and low leaf-freezing resistance (Fig. 3; see *Methods* for details). This suggested that 51 and 35% of European and 35 and 26% of Asian shrubland and temperate forest area, respectively, may increasingly be threatened by late-frost damage, whereas only 7 and 10% of the shrubland and forest area in North America are likely to be increasingly threatened (Fig. 5) (similar results were obtained when using −4 °C as freezing threshold; *SI Appendix*, Fig. S7). In temperate coastal and eastern Europe and parts of Asia—where LSFs are now strongly increasing—the local woody species have opportunistic phenological strategies (early leaf-out and high interannual leaf-out variation; Fig. 4 and refs. 29–31) and low leaf-freezing resistance (Fig. 3), suggesting an increasing mismatch between future LSFs and species' innate resistance strategies.

Our plant trait maps, based on common-garden data, must largely reflect genetic differences in leaf-out phenology and leaf-freezing resistance because woody plants in botanical gardens have no opportunity to reproduce, experience selection, and evolve local adaptations. The absence of natural populations in gardens also means that we cannot draw conclusions about population-level trait variability. Our results, however, are robust against effects of within-species phenological variation because we studied leaf-out in different individuals from eight botanical gardens throughout the Northern Hemisphere, and species-level differences in leaf-out phenology have been shown to be consistent across locations (figure 3 in ref. 33). The strong phylogenetic signal in leaf-out phenology (30) also implies that within-species variation is small compared with the interspecific variability observed across our global 1,500-species sample. So far, there is no evidence for population-level variation in leaf-freezing resistance (17), but an important avenue for future work is how freezing resistance changes during organ development. In a few species where this has been studied, freezing resistance is lowest shortly after spring bud break and increases as leaves mature (20).

Our results show that biogeographic differences in LSF have left important legacies in the growth strategies of temperate woody plants and imply that mismatches between past and future late-frost occurrences may cause a disequilibrium between climate conditions and species' leaf-out strategies and freezing resistance (34, 35). The mapped trait data and spring-frost occurrence of the past 58 y also allow detecting forest regions that seem especially vulnerable to early-season frost damage if current climate trends continue. Ultimately, the results may help guide decision-making in land management, forestry, agriculture, and insurance policy.

Methods

Computation of LSF. A late-frost event in spring is defined as freezing occurring after a substantial amount of warming has already accumulated, exposing emerging plant tissue to frost. Following this definition, we calculated LSF as the accumulating warming before the last spring freezing event in any given year. The more warming has occurred before the last frost, the further along leaf or flower development, making these organs more susceptible to freezing temperatures. To quantify the accumulated warming before the last frost, we used growing-degree days, calculated as the sum of daily degree days (above 0 °C) from 1 January (for the Northern Hemisphere) or 1 July (for the Southern Hemisphere) until the last frost day in spring (daily minimum temperatures below 0 °C). Organismic tissue, such as plant leaves, often can resist temperatures slightly below 0 °C (17, 20, 36). However, radiative cooling during clear and windless nights can cause temperatures in plant tissues to fall several degrees below measured air temperatures (37). Thus, it is common to observe late-frost damage in trees when the measured dry air temperature is close to 0 °C (27). Nevertheless, to evaluate the robustness of our results, we also analyzed LSF using −4 °C as freezing threshold (referred to as extreme LSF). This did not change the results (*SI Appendix*, Fig. S1 *A*, *C*, and *E*). The analysis was carried out for the four biomes to which our LSF measure applies: temperate shrubland, temperate broadleaf/mixed forest, temperate conifer forest, and boreal forests. The spatial distribution of biomes followed ref (38). Temperature data at 0.5° spatial resolution between 1959 and 2017 were taken from the Climate Research Unit/National Center for Atmospheric Research time-series dataset (https://crudata.uea.ac.uk/cru/data/ncep/). Daily mean temperatures were used to calculate degree days; daily minimum temperatures were used to determine the occurrence of freezing events.

To explore geographic differences in LSF, for each pixel, we calculated the 95% quantile of accumulated growing-degree days before the last frost between 1959 and 2017. This measure reflects the spatial variation in LSF due to extreme years. To test for the robustness of our measure, we additionally calculated LSF using 50% quantiles of accumulated warming, a degree-day threshold of 5 °C, or a freezing threshold of −4 °C, which did not change the results (*Methods* and *SI Appendix*, Fig. S1). Specifically, spatial LSF remained similar when 1) using a growing-degree day threshold of 5 °C, instead of 0 °C (Pearson's $r = 0.94$); 2) using a freezing threshold of −4 °C, instead of 0 °C (Pearson's r across all pixels = 0.86 and see *SI Appendix*, Fig. S1*E* for correlation coefficients per biome and continent); and 3) calculating the mean instead of the 95% quantile of accumulated growing-degree days before the last frost between 1959 and 2017 (Pearson's $r = 0.94$). To validate that our measure of LSF captures the actual frost risk experienced by plants over time, in *SI Appendix*, Fig. S2, we show deviations from average LSF for regions and years known to have suffered from exceptional late-frost events (24, 39, 40).

To analyze temporal changes in LSF, we used 10-y moving windows and calculated the maximum growing-degree days accumulating before the last frost for each 10-y period to reflect extreme years. Linear regression and Mann–Kendall trend analysis (41, 42) were applied to test for the magnitude and direction of temporal changes of LSF (referred to as "LSF change"). Whether or not the spatial distribution of LSF change was similar between the two applied freezing thresholds (0 and −4 °C) depended on continent and biome (*SI Appendix*, Figs. S1*F* and S3; Pearson's *r* across all pixels: 0.12). While in Europe and Asia, measures were positively correlated with each other (Pearson's $r = 0.05$ to 0.44), they tended to be negatively correlated in North America (Pearson's $r = -0.20$ to −0.01; *SI Appendix*, Fig. S1*F*). We also calculated LSF change using 5 °C (instead of 0 °C) as growing-degree day threshold and obtained similar spatial patterns (Pearson's $r = 0.95$). The same results were also obtained when calculating the mean (instead of the maximum) degree days before the last frost for each 10-y period (Pearson's $r = 0.65$). However, regional LSF risk is determined by extreme years, not the "average year," and thus, in this study, we exclusively focus on the maximal warming before the last frost within each 10-y period to calculate temporal LSF trajectories.

We tested six climate and topographic variables for their relationship with LSF and LSF change (Fig. 2): intramonthly temperature variation (Temp IMV), temperature seasonality, absolute latitude, easting, distance to the sea, and elevation. Temp IMV and temperature seasonality were extracted from the Worldclim dataset (43). Temp IMV is calculated as the mean of the differences between monthly maximum and minimum temperatures (BIO2) and thus reflects the average temperature variation that occurs within a month. Temperature seasonality is the difference in degrees Celsius between the maximum temperature of the warmest month and the minimum temperature of the coldest month (BIO7). To explore which variables best explain spatial variation in LSF within biomes, we ran univariate and multivariate ordinary least-squares regression models for each of the four biome types, temperate grass-/shrubland, temperate broadleaf/mixed forest, conifer forest, and boreal forest. Among all predictor variables, the Pearson correlation coefficients were below 0.5 and the variance inflation factors were below 4, indicating sufficient independence among covariates. We additionally tested for continental differences in LSF by running univariate models, including each continent as a binary variable of whether a pixel is present in the respective continent or not. To examine relative effect sizes, all variables were standardized by subtracting their mean and dividing by 2 SD before analysis (44).

Plant Traits Governing the Susceptibility to LSF. As a measure of the variation among species in their genetically determined leaf-out times, we used common garden leaf-out data for 1,455 deciduous angiosperms and 113 evergreen conifers observed in spring 2012 at eight Northern Hemisphere gardens located in Eastern North America, Europe, and East Asia (33, 45) (Dataset S1). On average, two individuals were observed for each species. For each species, we calculated a single average leaf-out date based on all available garden observations. Not all species were shared between sites, and we accounted for this by applying site-based corrections (45). First, a site-adjustment factor for each site was calculated across species as the difference between the mean leaf-out date at the respective site and the

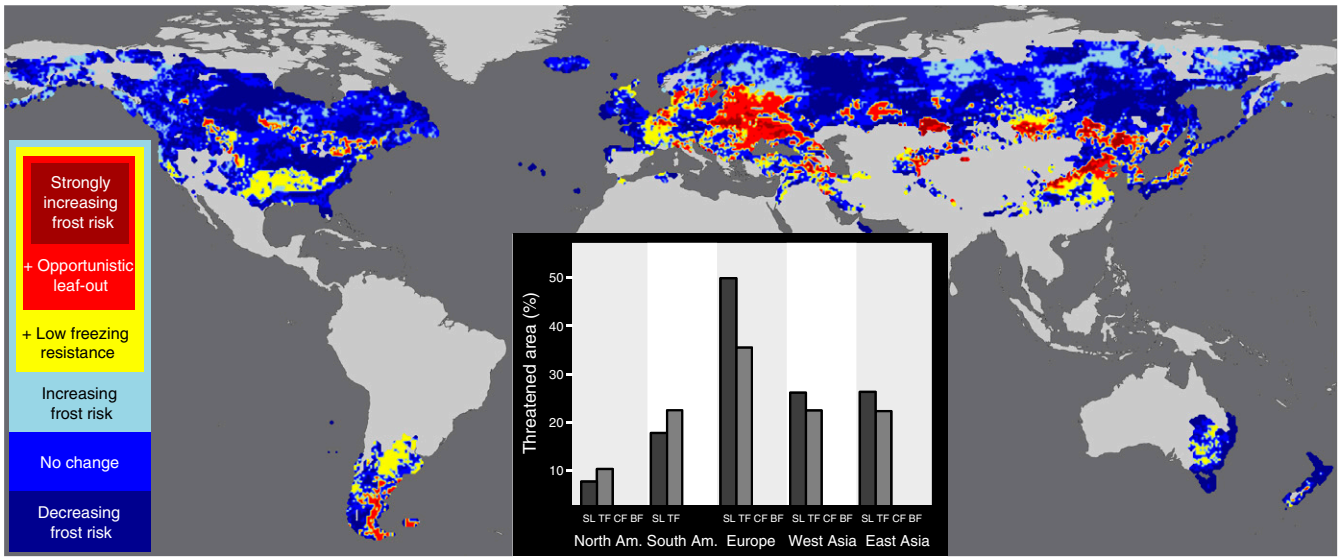

Fig. 5. Temporal changes in tree frost-damage risk, integrating climate and plant-trait information. Red areas are of particular concern. In those areas, LSF is significantly increasing over time (Fig. 1*B*), and woody plants growing there are evolutionarily not well-equipped to withstand LSFs because their leaves have low freezing resistance (Fig. 3) and their phenology is opportunistic, i.e., they leaf-out earlier and respond more strongly to temperature changes compared with plants from other regions when observed under common-garden conditions (Fig. 4). "Decreasing frost risk": significantly decreasing LSF over time; "No change": no significant change in LSF over time; "Increasing frost risk": significantly increasing LSF over time; "+ Low leaf-freezing resistance": increasing LSF and leaf-freezing resistance <75%; "+ Opportunistic leaf-out": increasing LSF, leaf-freezing resistance <75%, average leaf-out date <108, and average leaf-out variation ≥9; "Strongly increasing frost risk": LSF increasing by >30 growing-degree days per decade, leaf-freezing resistance <50%, average leaf-out date <108, and average leaf-out variation ≥9. *Inset* shows the relative area per continent and biome that falls in the last two categories. BF, boreal forest; CF, temperate conifer forest; SL, shrubland; TF, temperate forest (broadleaf/mixed).

mean leaf-out date across all sites. Second, adjusted leaf-out dates were calculated by adding the respective adjustment factor to a species' leaf-out date at each site. Finally, species-specific leaf-out dates were obtained by averaging the adjusted leaf-out dates across sites. Leaf-out dates of species averaged across sites closely mirror species leaf-out dates at individual sites (average R^2 = 0.80; figure 3 in ref. 33), highlighting the strong genetic component of leaf-out.

To determine species' spring temperature sensitivity (i.e., the extent to which their leaf-out is determined by air temperatures), we used data on 414 deciduous woody species studied over 6 y (2012 to 2017) in the Munich Botanical Garden. Spring temperatures in Munich during 2012 to 2017 showed high interannual variation, with the year 2016 being the warmest year recorded since 1888, and the year 2013 being among the five coldest years recorded since 1888. As a proxy for spring temperature sensitivity, we calculated the SD of these species' yearly leaf-out dates (Dataset S2). Species that respond to spring warming can be expected to show high interannual leaf-out variation, whereas species in which leaf-out is constrained by factors other than spring temperature, such as chilling and day length, show low interannual variation (46). Since all trees of the 414 species were observed under common conditions in a single garden, this measure then allowed us to compare their intrinsic, genetically determined responses.

Data on leaf-freezing resistance in individuals from 314 deciduous woody species and 40 evergreen conifers came from personal observations in the Munich Botanical Garden from 2012 to 2018 and ref. 40 (Dataset S3). During winter/spring, trees and shrubs were regularly (two times per week) inspected for leaf-out and leaf-freezing damage (recorded as percentage of damaged leaves per plant), and this information was then matched with the minimum temperature occurring during the preceding nights. On average, two individuals were observed per species, but within-species variation was generally low, and in no case did we observe a significant difference in freezing resistance among individuals of the same species. This allowed us to score the percentage of leaf frost damage with respect to preceding minimum temperatures; for example, on 20 March 2018, a minimum temperature of −8.2 °C was observed, and for plants that had already leafed out, we could record the leaf damage caused by −8.2 °C. Significant late-frost events also occurred on 27 April 2016 (−1.4 °C) and 20 April 2017 (−2.6 °C). Of course, only individuals that had already developed leaves when the frost occurred could be scored for leaf-freezing damage. To be consistent with ref. 40, for each species, we transferred our data to a binary variable, scoring for each species whether frost damage occurs in >50% of leaves at temperatures below −4 °C. To reflect the actual minimum temperatures perceived by plants, we measured hourly temperatures at 2-m height with Hobo data loggers installed without shelter protection (Onset Computer Corp.). As expected, the obtained minimum temperatures were significantly lower compared with weather-station air temperatures under the sheltered conditions of a Stevenson screen (e.g., 20 April 2016: −1.4 °C versus +0.6 °C; 20 March 2018: −8.2 °C versus −5.8 °C).

Spatial Mapping of Plant Traits and Their Interaction with LSF. We quantified the average leaf-out strategy (leaf-out date and interannual leaf-out variation from common-garden observations; see above) and leaf-freezing resistance across >0.5 million temperate and boreal forest inventory plots included in the Global Forest Biodiversity initiative (GFBi) database (47–49). The GFBi database consists of individual-based data compiled from all of the regional and national GFBi forest-inventory datasets, including the French and Italian National Forest Inventory (NFI) (50, 51). The average plot size is 1 ha. The standardized GFBi data frame (that is, tree list) comprises tree identifier (ID) (a unique number assigned to each individual tree); plot ID (a unique string assigned to each plot); plot coordinates, in decimal degrees of the WGS84 datum; tree size, in diameter-at-breast-height; trees-per-hectare expansion factor; year of measurement; dataset name (a unique name assigned to each forest inventory dataset); and binomial species names of trees. To prevent mismatches between the GFBi database and our trait data due to ambiguous taxonomy and spelling errors, binomial species names were cleaned using the Taxonomic Name Resolution Service platform (52). We only kept plots for which we had trait information on more than 50% of their individuals. For broadleaf forests and shrublands, we excluded plots with trait data on fewer than three species. For conifer and boreal forests, no such filtering was applied because monospecific populations are common in evergreen coniferous forests. Next, we obtained a single trait value for each plot, by calculating the trait mean of all species occurring in the respective plot. To match the spatial resolution of our LSF map, plot-level values were aggregated to the 50 × 50 km pixel level by averaging across all plots within a pixel, to generate 4,408 unique pixel locations across the world (*SI Appendix*, Fig. S4 and Table S1).

To extrapolate the global distribution of tree leaf-out strategy and leaf-freezing resistance across the world's temperate and boreal regions and

identify factors determining spatial variation in these traits, we assembled 10 global predictor layers: seven climate variables (LSF, mean annual temperature, temperature seasonality, intramonthly temperature variation, mean annual precipitation, precipitation seasonality, and mean annual solar radiation) and three topographic variables (elevation, distance to the sea, and easting). We implemented the random-forest algorithm (32) using the H_2O-package (version 3.26.0.2) in R. Random-forest fits a large set of regression trees, each one fitted on a random subset of the data, and each split based on a random subset of the predictors. A prediction for any given case is given by the mode of the predictions for that case across all regression trees. Models were run separately for each biome, grass/shrubland, broadleaf/mixed forest, conifer forest, and boreal forest. Model fit was evaluated by computing R^2 values based on the correlation between observed and predicted values. To test the sensitivity of model predictions to losing random subsets from the training data, we performed 10-fold cross-validation tests (*SI Appendix*, Fig. S5). Because evergreen conifers leaf-out drastically later than broadleaf trees, we do not show both predictions in the same map for clarity (Fig. 4 and *SI Appendix*, Fig. S8).

To explore which variables best explain spatial variation in leaf-out strategy and leaf-freezing resistance within biomes, we additionally ran univariate ordinary least-squares regression models, standardizing both predictor and response variables (*SI Appendix*, Fig. S6). To obtain a more comprehensive analysis of the relationship between LSF and leaf-out strategy, we applied quantile regression analysis, using the quantreg-package (version 5.35) in R. Specifically, this allowed us to test whether there is cautious leaf-out in regions with severe LSFs, whereas leaf-out strategies might be more dispersed in low LSF regions (indicating that factors aside from late frost have shaped phenological strategies in low LSF regions) (Fig. 4 *C* and *D*). To exclude covariate effects of latitude, we additionally tested for the effects of LSF on leaf-out strategy controlling for absolute latitude, using partial regression analysis implemented in the car-package (version 3.0.0) in R (Fig. 4 *C* and *D*, *Insets*).

To map the geographic distribution of temporal changes in the sensitivity of trees to late-frost damage, in Fig. 5 and *SI Appendix*, Fig. S7, we show maps that integrate temporal changes in abiotic LSF (Fig. 1*C*) with information on species' phenological strategy (Fig. 4) and leaf-freezing resistance (Fig. 3). Each $0.5 \times 0.5°$ pixel was assigned to a late-frost damage risk category, where blue pixels indicate no change or decreasing late-frost damage risk and yellow to red areas indicate an increasing threat of frost damage. Temporal changes in late-frost damage risk using 0 and −4 °C as freezing thresholds are shown in Fig. 5 and *SI Appendix*, Fig. S7, respectively. In the dark blue pixels, abiotic LSF is significantly decreasing over time; in the blue pixels, LSF is not significantly changing over time. In all other pixels, abiotic LSF is significantly increasing over time. However, some regions might be well equipped to withstand more severe LSFs because they harbor trees with high freezing resistance and cautious phenologies. To account for this, light blue pixels in Fig. 5 and *SI Appendix*, Fig. S7 indicate areas that harbor a high proportion of trees with high leaf-freezing resistance (≥75%; Fig. 3) and with cautious phenologies, i.e., trees, on average, leaf-out late (day-of-year ≥108; Fig. 4*A*) and respond only little to temperature changes (SD < 9; Fig. 4*B*) when observed under common-garden observations. The phenology thresholds (day of year: 108; SD: 9) were chosen based on the means of all species in our dataset. Yellow areas harbor trees with low leaf-freezing resistance (<75%) but cautious phenologies. Red and dark red areas (in Fig. 5 and *SI Appendix*, Fig. S7) harbor a high proportion of trees with both low leaf-freezing resistance and opportunistic phenologies (with an average leaf-out date of <108 and an average leaf-out variation of ≥9) and thus are of particular concern. In the dark red areas, trees have low leaf-freezing resistance (<50%), and abiotic LSF is strongly increasing (by >30 growing-degree days per decade; Fig. 1*B*). All statistical analyses were conducted in R (version 3.4.1) (53).

Data Availability. The trait data used for this study is available in Datasets S1–S3. All source code, models, and raw data are available at https://github.com/LidongMo/FrostRiskProject.

ACKNOWLEDGMENTS. This work was supported by the ETH Zurich Postdoctoral Fellowship Program (C.M.Z.); the China Scholarship Council (L.M.); Deutsche Forschungsgemeinschaft Grant RE 603/25-1 (to S.S.R.); and DOB Ecology, Plant-for-the-Planet, and the German Federal Ministry for Economic Cooperation and Development (T.W.C.). J.-C.S. considers this work a contribution to his Villum Investigator Project "Biodiversity Dynamics in a Changing World," funded by Villum Fondon Grant 16549, and his Natural Sciences Project "Tree Diversity Dynamics under Climate Change," funded by Independent Research Fund Denmark Grant 6108-00078B. A.O. was supported by both Aarhus University Research Foundation (AUFF) Starting Grant AUFF-F-201 8-7-8 and H2020 Marie Skłodowska-Curie Actions Grant/Award 748753; T.M.F. was supported by European Research Council Advanced Grant 669609; and A.M.J. was supported by the General Directorate of State Forests, Warsaw, Poland (Research Projects No. 1/07 and OR/2717/3/11). We thank the following agencies, initiatives, teams, and individuals for forest inventory data collection and financial or other technical support: the United States Department of Agriculture (USDA); the Forest Service; the Forest Inventory and Analysis Program; the University of Alaska Fairbanks; the USDA National Institute of Food and Agriculture McIntire–Stennis Projects (accession no. 1017711); the NFI of Canada; the Ministère des Forêts, de la Faune et des Parcs du Québec (Canada); the Natural Sciences and Engineering Research Council of Canada; and the Department of Biotechnology, the Government of India, through the project "Mapping and Quantitative Assessment of Geographic Distribution and Population Status of Plant Resources of Eastern Himalayan Region" (reference no. BT/PR7928/NDB/52/9/2006, dated 29 September 2006) for financial support; all persons who made the Third Spanish Forest Inventory possible, especially to the Área de Inventario y Estadísticas Forestales for facilitating the access to forest inventory data; the Thünen Institute of Forest Ecosystems (Germany) for providing NFI data; the Swiss, Italian, and French NFI for the work done to make forest inventory data publicly available; Instituto de Conservação da Natureza e Florestas–Dados do Inventário Florestal Nacional; and the state assignment of "Methodical Approaches to the Assessment of the Structural Organization and Functioning of Forest Ecosystems" (no. AAAA-A18-118052400130-7) for data collection in Russia.

[a]Institute of Integrative Biology, ETH Zurich (Swiss Federal Institute of Technology), 8092 Zurich, Switzerland; [b]Systematic Botany and Mycology, Department of Biology, Ludwig Maximilian University of Munich, 80638 Munich, Germany; [c]Center for Biodiversity Dynamics in a Changing World (BIOCHANGE), Department of Biology, Aarhus University, DK-8000 Aarhus C, Denmark; [d]Section for Ecoinformatics and Biodiversity, Department of Biology, Aarhus University, DK-8000 Aarhus C, Denmark; [e]Swiss Federal Institute for Forest, Snow and Landscape Research WSL, CH-8903 Birmensdorf, Switzerland; [f]Department of Biological Sciences, University of Bergen, 5020 Bergen, Norway; [g]Copernicus Institute of Sustainable Development, University of Utrecht, 3584 CS Utrecht, The Netherlands; [h]Computational and Applied Vegetation Ecology Lab, Department of Applied Ecology and Environmental Biology, Faculty of Bioscience Engineering, Ghent University, Ghent 9000, Belgium; [i]Department of Forest Resources, University of Minnesota, St. Paul, MN 55108; [j]Hawkesbury Institute for the Environment, Western Sydney University, Penrith NSW 2753, Australia; [k]Lab of Forest Advanced Computing and Artificial Intelligence, Department of Forestry and Natural Resources, Purdue University, West Lafayette, IN 47907; [l]Wageningen Environmental Research, Wageningen University and Research, 6700AA, Wageningen, The Netherlands; [m]Forest Ecology and Forest Management, Wageningen University and Research, 6700AA, Wageningen, The Netherlands; [n]Department of Crop and Forest Sciences, University of Lleida, E25198 Lleida, Spain; [o]Joint Research Unit, Forest Science and Technology Centre of Catalonia CTFC–Centre for Research in Agrotechnology, E25280, Solsona, Spain; [p]Department of Agricultural, Food, Environmental and Animal Sciences, University of Udine, 33100 Udine, Italy; [q]Institute of BioEconomy, National Research Council, 50019 Florence, Italy; [r]Division of Forestry and Forest Resources NIBIO, Norwegian Institute of Bioeconomy Research, NO-1431 Ås, Norway; [s]Department of Geomatics, Forest Research Institute, Sekocin Stary, 05-090 Raszyn, Poland; [t]Swiss National Forest Inventory, Swiss Federal Institute for Forest, Snow and Landscape Research WSL, CH-8903 Birmensdorf, Switzerland; [u]Faculty of Natural Resources Management, Lakehead University, Thunder Bay, ON P7B 5E1, Canada; [v]Key Laboratory for Humid Subtropical Eco-geographical Processes of the Ministry of Education, School of Geographical Sciences, Fujian Normal University, 350117 Fujian, China; [w]Institute of Forest Ecosystem Research IFER, CZ 254 01 Jilove u Prahy, Czech Republic; [x]Global Change Research Institute, Czech Academy of Sciences, CZ 603 00 Brno, Czech Republic; [y]Centre for Structural and Functional Genomics, Biology Department, Concordia University, Montreal, QC H4B 1R6, Canada; [z]Quebec Centre for Biodiversity Science, Biology Department, Concordia University, Montreal, QC H4B 1R6, Canada; [aa]Biology Centre of the Czech Academy of Sciences, Institute of Entomology, 370 05 Ceske Budejovice, Czech Republic; [bb]Institute for Tropical Biology and Conservation, Universiti Malaysia Sabah, 88400 Kota Kinabalu, Sabah, Malaysia; [cc]Department of Sustainable Agro-ecosystems and Bioresources, Research and Innovation Centre, Fondazione Edmund Mach, 38010 San Michele all'Adige, Trentino, Italy; [dd]Institute of Dendrology, Polish Academy of Sciences, PL-62-035 Kórnik, Poland; [ee]Faculty of Forestry, Department of Game Management and Forest Protection, Poznan University of Life Sciences, PL-60-625 Poznan, Poland; [ff]Białowieża Geobotanical Station, Faculty of Biology, University of Warsaw, PL-17-230 Bialowieza, Poland; [gg]School of Biological Sciences, University of Bristol, Bristol, BS8 1TQ United Kingdom; [hh]Department of Geosciences and Natural Resource Management, University of Copenhagen, Frederiksberg C 1958, Denmark; [ii]Department of Botany, Dr. Harisingh Gour Vishwavidyalaya University, Sagar, Madhya Pradesh 470003, India; [jj]Department of Forest

Sciences, Seoul National University, 08826 Seoul, Republic of Korea; [kk]Interdisciplinary Program in Agricultural and Forest Meteorology, Seoul National University, 08826 Seoul, Republic of Korea; [ll]National Center for Agro Meteorology, 08826 Seoul, Republic of Korea; [mm]Research Institute for Agriculture and Life Sciences, Seoul National University, 08826 Seoul, Republic of Korea; [nn]Institute of Forestry and Rural Engineering, Estonian University of Life Sciences, 51006 Tartu, Estonia; [oo]Tartu Observatory, University of Tartu, 61602 Tõravere, Estonia; [pp]Coordination Centre for Environmental Projects, Polish State Forests, 02-362 Warsaw, Poland; [qq]Department of Evolutionary Biology and Environmental Studies, University of Zurich, 8057 Zurich, Switzerland; [rr]Centre for Forest Research, Université du Québec à Montréal, Montreal, H3C 3P8 Canada; [ss]School of Life Sciences Weihenstephan, Technical University of Munich, 85354 Freising, Germany; [tt]Department of Environmental Sciences, Central University of Jharkhand, Brambe, Ranchi, Jharkhand 835205, India; [uu]Silviculture and Forest Ecology of the Temperate Zones, University of Göttingen, 37077 Göttingen, Germany; [vv]National Forest Centre, 96001 Zvolen, Slovak Republic; [ww]Faculty of Forestry and Wood Sciences, Czech University of Life Sciences in Prague, Praha 6 Suchdol, 16521, Czech Republic; [xx]Center for Forest Ecology and Productivity, Russian Academy of Sciences, 117997 Moscow, Russian Federation; [yy]Agricultural High School, Polytechnic Institute of Viseu, 3500-606 Viseu, Portugal; [zz]Centre for the Research and Technology of Agro-Environmental and Biological Sciences, Universidade de Trás-os-Montes e Alto Douro, Quinta de Prados, 5000-801 Vila Real, Portugal; and [aaa]Research Center of Forest Management Engineering of State Forestry and Grassland Administration, Beijing Forestry University, 100083 Beijing, China

1. M. Reichstein *et al*., Climate extremes and the carbon cycle. *Nature* **500**, 287–295 (2013).
2. P. Ciais *et al*., Europe-wide reduction in primary productivity caused by the heat and drought in 2003. *Nature* **437**, 529–533 (2005).
3. C. C. Ummenhofer, G. A. Meehl, Extreme weather and climate events with ecological relevance: A review. *Philos. Trans. R. Soc. Lond. B Biol. Sci.* **372**, 20160135 (2017).
4. D. B. Lobell, W. Schlenker, J. Costa-Roberts, Climate trends and global crop production since 1980. *Science* **333**, 616–620 (2011).
5. C. B. Field, V. Barros, T. F. Stocker, Q. Dahe, *Managing the Risks of Extreme Events and Disasters to Advance Climate Change Adaptation: Special Report of the Intergovernmental Panel on Climate Change*, (Cambridge University Press, 2012).
6. C. Rosenzweig, A. Iglesias, X. B. Yang, P. R. Epstein, E. Chivian, Climate change and extreme weather events; implications for food production, plant diseases, and pests. *Glob. Change Hum. Health* **2**, 90–104 (2001).
7. T. Jeworrek, "Media Information Extreme storms, wildfires and droughts cause heavy nat cat losses in 2018" (2019). https://www.google.com/url?sa=t&rct=j&q=&esrc=s&source=web&cd=2&ved=2ahUKEwjO__z0wvzoAhWN3KQKHY5hDGQQFjABegQIAxAB&url=https%3A%2F%2Fwww.munichre.com%2Fcontent%2Fdam%2Fmunichre%2Fglobal%2Fcontent-pieces%2Fdocuments%2Fnatcat-2018-global-20190107_en.pdf%2F_jcr_content%2Frenditions%2Foriginal.media_file.download_attachment.file%2Fnatcat-2018-global-20190107_en.pdf&usg=AOvVaw0_lO6uW9VTJ0As1EcE6K0y. Accessed 27 April 2020.
8. S. Hallegatte, J. C. Hourcade, P. Dumas, Why economic dynamics matter in assessing climate change damages: Illustration on extreme events. *Ecol. Econ.* **62**, 330–340 (2007).
9. P. Stott, How climate change affects extreme weather events. *Science* **352**, 1517–1518 (2016).
10. C. Körner *et al*., Where, why and how? Explaining the low-temperature range limits of temperate tree species. *J. Ecol.* **104**, 1076–1088 (2016).
11. C. Kollas, C. Körner, C. F. Randin, Spring frost and growing season length co-control the cold range limits of broad-leaved trees. *J. Biogeogr.* **41**, 773–783 (2014).
12. Q. Liu *et al*., Extension of the growing season increases vegetation exposure to frost. *Nat. Commun.* **9**, 426 (2018).
13. A. Príncipe *et al*., Low resistance but high resilience in growth of a major deciduous forest tree (Fagus sylvatica L.) in response to late spring frost in southern Germany. *Trees (Berl.)* **31**, 743–751 (2017).
14. C. M. Zohner, A. Rockinger, S. S. Renner, Increased autumn productivity permits temperate trees to compensate for spring frost damage. *New Phytol.* **221**, 789–795 (2019).
15. C. K. Augspurger, Reconstructing patterns of temperature, phenology, and frost damage over 124 years: Spring damage risk is increasing. *Ecology* **94**, 41–50 (2013).
16. Y. Vitasse *et al*., Contrasting resistance and resilience to extreme drought and late spring frost in five major European tree species. *Glob. Change Biol.* **25**, 3781–3792 (2019).
17. Y. Vitasse, A. Lenz, C. Körner, The interaction between freezing tolerance and phenology in temperate deciduous trees. *Front. Plant Sci.* **5**, 541 (2014).
18. C. M. Zohner, L. Mo, V. Sebald, S. S. Renner, Leaf-out in northern ecotypes of wide-ranging trees requires less spring warming, enhancing the risk of spring frost damage at cold range limits. *Glob. Ecol. Biogeogr.*, doi.org/10.1111/geb.13088 (2020).
19. A. Vitra, A. Lenz, Y. Vitasse, Frost hardening and dehardening potential in temperate trees from winter to budburst. *New Phytol.* **216**, 113–123 (2017).
20. A. Lenz, G. Hoch, Y. Vitasse, C. Körner, European deciduous trees exhibit similar safety margins against damage by spring freeze events along elevational gradients. *New Phytol.* **200**, 1166–1175 (2013).
21. R. L. Snyder, J. de Melo-Abreu, *Frost Protection: Fundamentals, Practice and Economics*, (Cambridge University Press, 2005).
22. K. Papagiannaki, K. Lagouvardos, V. Kotroni, G. Papagiannakis, Agricultural losses related to frost events: Use of the 850 hPa level temperature as an explanatory variable of the damage cost. *Nat. Hazards Earth Syst. Sci.* **14**, 2375–2381 (2014).
23. E. Faust, J. Herbold, *Spring Frost Losses and Climate Change–Not a Contradiction in Terms*, (Munich RE, 2018).
24. K. Hufkens *et al*., Ecological impacts of a widespread frost event following early spring leaf-out. *Glob. Change Biol.* **18**, 2365–2377 (2012).
25. M. Bascietto, S. Bajocco, F. Mazzenga, G. Matteucci, Assessing spring frost effects on beech forests in Central Apennines from remotely-sensed data. *Agric. For. Meteorol.* **248**, 240–250 (2018).
26. A. D. Richardson *et al*., Ecosystem warming extends vegetation activity but heightens vulnerability to cold temperatures. *Nature* **560**, 368–371 (2018).
27. Y. Vitasse, L. Schneider, C. Rixen, D. Christen, M. Rebetez, Increase in the risk of exposure of forest and fruit trees to spring frosts at higher elevations in Switzerland over the last four decades. *Agric. For. Meteorol.* **248**, 60–69 (2018).
28. C. J. Chamberlain, B. I. Cook, I. García de Cortázar-Atauri, E. M. Wolkovich, Rethinking false spring risk. *Glob. Chang. Biol.* **25**, 2209–2220 (2019).
29. C. M. Zohner, S. S. Renner, Innately shorter vegetation periods in North American species explain native-non-native phenological asymmetries. *Nat. Ecol. Evol.* **1**, 1655–1660 (2017).
30. C. M. Zohner, B. M. Benito, J. D. Fridley, J. C. Svenning, S. S. Renner, Spring predictability explains different leaf-out strategies in the woody floras of North America, Europe and East Asia. *Ecol. Lett.* **20**, 452–460 (2017).
31. C. Körner, D. Basler, Phenology under global warming. *Science* **327**, 1461–1462 (2010).
32. L. Breiman, Random forests. *Mach. Learn.* **45**, 5–32 (2001).
33. E. Desnoues, J. Ferreira de Carvalho, C. M. Zohner, T. W. Crowther, The relative roles of local climate adaptation and phylogeny in determining leaf-out timing of temperate tree species. *For. Ecosyst.* **4**, 26 (2017).
34. J. C. Svenning, B. Sandel, Disequilibrium vegetation dynamics under future climate change. *Am. J. Bot.* **100**, 1266–1286 (2013).
35. S. S. Renner, C. M. Zohner, Climate change and phenological mismatch in trophic interactions among plants, insects, and vertebrates. *Annu. Rev. Ecol. Evol. Syst.* **49**, 165–182 (2018).
36. Y. Vitasse, A. Lenz, G. Hoch, C. Körner, Earlier leaf-out rather than difference in freezing resistance puts juvenile trees at greater risk of damage than adult trees. *J. Ecol.* **102**, 981–988 (2014).
37. R. Leuning, K. W. Cremer, Leaf temperatures during radiation frost Part I. Observations. *Agric. For. Meteorol.* **42**, 121–133 (1988).
38. D. M. Olson *et al*., Terrestrial ecoregions of the world: A new map of life on earth. *Bioscience* **51**, 933–938 (2001).
39. L. Gu *et al*., The 2007 eastern US spring freeze: Increased cold damage in a warming world? *Bioscience* **58**, 253–262 (2008).
40. L. Muffler *et al*., Distribution ranges and spring phenology explain late frost sensitivity in 170 woody plants from the Northern Hemisphere. *Glob. Ecol. Biogeogr.* **25**, 1061–1071 (2016).
41. H. B. Mann, Nonparametric tests against trend. *Econometrica* **13**, 245–259 (1945).
42. M. G. Kendall, *Rank Correlation Methods*, (Griffin, 1948).
43. S. E. Fick, R. J. Hijmans, WorldClim 2: New 1-km spatial resolution climate surfaces for global land areas. *Int. J. Climatol.* **37**, 4302–4315 (2017).
44. A. Gelman, J. Hill, *Data Analysis Using Regression and Multilevel/hierarchical Models*, (Cambridge University Press, 2007).
45. Z. A. Panchen *et al*., Leaf out times of temperate woody plants are related to phylogeny, deciduousness, growth habit and wood anatomy. *New Phytol.* **203**, 1208–1219 (2014).
46. C. M. Zohner, B. M. Benito, J. C. Svenning, S. S. Renner, Day length unlikely to constrain climate-driven shifts in leaf-out times of northern woody plants. *Nat. Clim. Chang.* **6**, 1120–1123 (2016).
47. B. S. Steidinger *et al*.; GFBI consortium, Climatic controls of decomposition drive the global biogeography of forest-tree symbioses. *Nature* **569**, 404–408 (2019).
48. J. Liang *et al*., Positive biodiversity-productivity relationship predominant in global forests. *Science* **354**, aaf8957 (2016).
49. Ministerio de Medio Ambiente. Dirección General de Conservación de la Naturaleza. 1997–2007. Tercer Inventario Forestal Nacional. Gobierno de España. https://www.miteco.gob.es/es/biodiversidad/servicios/banco-datos-naturaleza/informacion-disponible/ifn3.aspx. Accessed 27 April 2020.
50. French National Forest Inventory, Data from "Institut National de l'information géographique et forestière, raw data, annual campaigns 2005 and following." https://inventaire-forestier.ign.fr/spip.php?rubrique159. Accessed 1 January 2015.
51. Italian National Forest Inventory, Data from "National Inventory of Forests and Forest Carbon Pools (INFC)." https://inventarioforestale.org/. Accessed 27 April 2016.
52. B. Boyle *et al*., The taxonomic name resolution service: An online tool for automated standardization of plant names. *BMC Bioinf.* **14**, 16 (2013).
53. R Development Core Team, R: A Language and Environment for Statistical Computing. R Foundation for Statistical Computing, Vienna, Austria (2017). http://www.R-project.org. Accessed 27 April 2020.